REPORT DOCUMENTATION PAGE

Form Approved OMB NO. 0704-0188

1. REPORT DATE (DD-MM-YYYY)	2. REPORT TYPE	3. DATES COVERED (From - To)
11-01-2008	Final Report	1-Aug-2004 - 31-Dec-2007

4. TITLE AND SUBTITLE
Modeling of Plasma Induced Ignition and Combustion

5a. CONTRACT NUMBER
W911NF-04-1-0251

5b. GRANT NUMBER

5c. PROGRAM ELEMENT NUMBER
611102

6. AUTHORS
Iain D. Boyd, Michael Keidar

5d. PROJECT NUMBER

5e. TASK NUMBER

5f. WORK UNIT NUMBER

7. PERFORMING ORGANIZATION NAMES AND ADDRESSES
University of Michigan - Ann Arbor
Office of Sponsored Programs
Room 1058 Wolverine Tower
Ann Arbor, MI 48109 -1274

8. PERFORMING ORGANIZATION REPORT NUMBER

9. SPONSORING/MONITORING AGENCY NAME(S) AND ADDRESS(ES)
U.S. Army Research Office
P.O. Box 12211
Research Triangle Park, NC 27709-2211

10. SPONSOR/MONITOR'S ACRONYM(S)
ARO

11. SPONSOR/MONITOR'S REPORT NUMBER(S)
44866-EG.1

12. DISTRIBUTION AVAILIBILITY STATEMENT
Approved for Public Release; Distribution Unlimited

13. SUPPLEMENTARY NOTES
The views, opinions and/or findings contained in this report are those of the author(s) and should not contrued as an official Department of the Army position, policy or decision, unless so designated by other documentation.

14. ABSTRACT
Much progress has been made in the work performed in this grant toward the development of an end-to-end computer model of an electrothermal chemical gun. Phenomena that must be considered in an electrothermal chemical gun model include the initial capillary plasma properties, the plasma-air interaction, plasma sheath effects, and the plasma-propellant interaction itself. This report presents an overview of our progress made modeling these various phenomena. Also discussed are methods under consideration to incorporate surface chemistry effects into the plasma-propellant interaction model.

15. SUBJECT TERMS
electrothermal chemical gun, ablation, plasma

16. SECURITY CLASSIFICATION OF:			17. LIMITATION OF ABSTRACT	15. NUMBER OF PAGES	19a. NAME OF RESPONSIBLE PERSON
a. REPORT	b. ABSTRACT	c. THIS PAGE			Iain Boyd
U	U	U	SAR		19b. TELEPHONE NUMBER 734-615-3281

Report Title

Modeling of Plasma Induced Ignition and Combustion

ABSTRACT

Much progress has been made in the work performed in this grant toward the development of an end-to-end computer model of an electrothermal chemical gun. Phenomena that must be considered in an electrothermal chemical gun model include the initial capillary plasma properties, the plasma-air interaction, plasma sheath effects, and the plasma-propellant interaction itself. This report presents an overview of our progress made modeling these various phenomena. Also discussed are methods under consideration to incorporate surface chemistry effects into the plasma-propellant interaction model.

List of papers submitted or published that acknowledge ARO support during this reporting period. List the papers, including journal references, in the following categories:

(a) Papers published in peer-reviewed journals (N/A for none)

Porwitzky, A.J., Keidar, M., and Boyd, I.D., "Modeling of the Plasma-Propellant Interaction," IEEE Transactions on Magnetics, Vol. 43, 2007, pp. 313-317.

Porwitzky, A.J., Keidar, M., and Boyd, I.D., “On the Mechanism of Energy Transfer in the Plasma-Propellant Interaction,” Propellants, Explosives, and Pyrotechnics, Vol. 32, 2007, pp. 385-391.

Keidar, M., Boyd, I.D., Williams, A. and Beyer, R., "Ablation Study in a Capillary Sustained Discharge," IEEE Transactions on Magnetics, Vol. 43, 2007, pp. 308-312.

Keidar, M. and Boyd, I.D., “Ablation Study in the Capillary Discharge of an Electrothermal Gun,” Journal of Applied Physics, Vol. 99, 2006, Article 053301.

Number of Papers published in peer-reviewed journals: 4.00

(b) Papers published in non-peer-reviewed journals or in conference proceedings (N/A for none)

Number of Papers published in non peer-reviewed journals: 0.00

(c) Presentations

Porwitzky, A.J., Scalabrin, L.C., Keidar, M., and Boyd, I.D., "Chemically Reacting Plasma Jet Expansion Simulation for Application to Electrothermal Chemical Guns," AIAA Paper 2007-4600, June 2007.

Number of Presentations: 1.00

Non Peer-Reviewed Conference Proceeding publications (other than abstracts):

Number of Non Peer-Reviewed Conference Proceeding publications (other than abstracts): 0

Peer-Reviewed Conference Proceeding publications (other than abstracts):

Number of Peer-Reviewed Conference Proceeding publications (other than abstracts): 0

(d) Manuscripts

Number of Manuscripts: 0.00

Number of Inventions:

Graduate Students

NAME	PERCENT_SUPPORTED
Andrew Porwitzky	1.00
FTE Equivalent:	**1.00**
Total Number:	**1**

Names of Post Doctorates

NAME	PERCENT_SUPPORTED
FTE Equivalent:	
Total Number:	

Names of Faculty Supported

NAME	PERCENT_SUPPORTED	National Academy Member
Iain Boyd	0.00	No
Michael Keidar	0.25	No
FTE Equivalent:	**0.25**	
Total Number:	**2**	

Names of Under Graduate students supported

NAME	PERCENT_SUPPORTED
FTE Equivalent:	
Total Number:	

Student Metrics

This section only applies to graduating undergraduates supported by this agreement in this reporting period

The number of undergraduates funded by this agreement who graduated during this period:	0.00
The number of undergraduates funded by this agreement who graduated during this period with a degree in science, mathematics, engineering, or technology fields:.....	0.00
The number of undergraduates funded by your agreement who graduated during this period and will continue to pursue a graduate or Ph.D. degree in science, mathematics, engineering, or technology fields:.....	0.00
Number of graduating undergraduates who achieved a 3.5 GPA to 4.0 (4.0 max scale):	0.00
Number of graduating undergraduates funded by a DoD funded Center of Excellence grant for Education, Research and Engineering:	0.00
The number of undergraduates funded by your agreement who graduated during this period and intend to work for the Department of Defense	0.00
The number of undergraduates funded by your agreement who graduated during this period and will receive scholarships or fellowships for further studies in science, mathematics, engineering or technology fields:	0.00

Names of Personnel receiving masters degrees

NAME
Andrew Porwitzky
Total Number: 1

Names of personnel receiving PHDs

NAME
Total Number:

Names of other research staff

NAME	PERCENT_SUPPORTED
FTE Equivalent:	
Total Number:	

Sub Contractors (DD882)

Inventions (DD882)

FINAL TECHNICAL REPORT
Modeling of Plasma-Induced Ignition and Combustion
ARO Grant W911NF-04-1-0251

Iain D. Boyd
Department of Aerospace Engineering, University of Michigan

***Abstract*— Much progress has been made in the work performed in this grant toward the development of an end-to-end computer model of an electrothermal chemical gun. Phenomena that must be considered in an electrothermal chemical gun model include the initial capillary plasma properties, the plasma-air interaction, plasma sheath effects, and the plasma-propellant interaction itself. This report presents an overview of recent progress made modeling these various phenomena. Also discussed are methods under consideration to incorporate surface chemistry effects into the plasma-propellant interaction model.**

***Index Terms*— capillary, ETC, heat flux, modeling, plasma, plasma chemistry, plasma sheath.**

I. Introduction

There has been much interest in recent years in the design and implementation of electrothermal chemical (ETC) guns. An ETC gun is a solid propellant based artillery piece in which the conventional ignition system is replaced with a capillary plasma source. Among the enhancements encountered in plasma based ignition systems are reduced ignition delay time, highly repeatable ignition time, and enhanced burning and combustion of the solid propellant [1], [2].

Work is continuing in the development of an end-to-end computer model of an ETC gun, focused primarily on modeling the physics of the plasma-propellant interaction. To date, models have been developed that address the capillary plasma source [3], [4], the plasma-air chemistry of the expanding capillary plasma jet into the combustion chamber [5], the plasma-propellant interaction via a coupled ablation and thermal model [6], and the convective heat flux to the propellant bed by means of a collisional plasma sheath model [7]. This effort represents the first attempt to create a model of the ETC phenomena, from the initial capillary firing through the plasma-propellant interaction leading up to propellant ignition.

In this report, we present an overview of the work done on the ETC model, including the major conclusions of the efforts. Section II addresses the capillary model. Section III summarizes CFD studies of the plasma-air interaction. The previously published plasma-propellant interaction model is covered in Section IV, which is loosely coupled to a collisional plasma sheath model described in Section V. A summary of current work on propellant surface chemistry is included in Section VI, with discussion on final model integration in Section VII. Concluding remarks are presented in Section VIII.

II. Capillary Model

The capillary model [3], [4] uses kinetic ablation theory for the wall material [8], [9], coupled to a non-equilibrium hydrodynamic layer. Solving the energy, momentum and mass conservation equations in the hydrodynamic layer allows for the determination of the plasma density and temperature at the polyethylene surface. The kinetic ablation model then determines the ablation rate, which in turn results in updated plasma density, pressure, and electron and surface temperatures.

The model is for a one dimensional axisymmetic capillary of length L and internal radius R. The spatial variable x varies from the back of the capillary to the exit plane, at $x = L$. The model assumes that all flow parameters are uniform along the radial direction in each layer. The energy equation in the hydrodynamic layer is

$$\rho \left(\frac{\partial \varepsilon}{\partial t} + U \frac{\partial \varepsilon}{\partial x} \right) = -P \frac{\partial U}{\partial x} + Q_j - Q_r - Q_F. \qquad (1)$$

Fluid density, velocity, and pressure are given by ρ, U and P, respectively. In (1), $\varepsilon = (3/2)(T/m) + (U^2/2)$, where T is the plasma temperature, and m is the mass of an average fluid particle. The influx of energy to the plasma due to Joule heating is represented by Q_j. Energy losses due to plasma radiation and convection to the wall are given by Q_r and Q_F, respectively. It is assumed, due to the high pressure and small scale of the capillary, that pressure is constant in the hydrodynamic layer, thus $\partial P/\partial x = 0$. Previous simulations and theoretical estimates indicate that the plasma temperature varies only slightly in the capillary, thus it is assumed that $\partial T/\partial x = 0$.[3]

Solving the energy, momentum and mass conservation equations in the hydrodynamic layer yields the following relation

for the ablation rate, Γ,

$$\Gamma = mn_1\sqrt{\frac{n_2kT_2 - n_1kT_1}{mn_1(1-n_1/n_2)}}, \quad (2)$$

where k is the Boltzmann constant and n is the fluid number density. Subscripts 1 and 2 represent values at the Knudsen/hydrodynamic layer and the hydrodynamic/quasi-neutral plasma layer boundaries, respectively [3]. Note that (2) is only real if $n_1kT_1 > n_2kT_2$ and $n_1 > n_2$. If these conditions are not met the implication is that the backflux is higher than the flux from the wall into the bulk plasma. When this is the case, deposition to the polyethylene surface takes place, and the total ablated mass decreases. Both conditions are met during the discharge, thus the capillary model accommodates both situations. Polyethylene, and therefore the capillary plasma, is composed of carbon and hydrogen. Studies of film deposition have shown that carbon is likely to deposit and accumulate on the surface, while hydrogen is not. To account for this the model includes a parameter ν, which is the fraction of the backflux that deposits on the surface, with $\nu = 1$ being the most deposition, and $\nu = 0$ neglecting deposition entirely. Previous simulations and experiments found good agreement with $\nu = 0.6$ [4].

As inputs the model requires capillary length and internal radius, a value for the backflux parameter ν, and a time varying electric current profile. Polynomial curve fits to experimentally measured discharge currents can be input into the model to attempt to match specific experimental data.

As outputs the capillary model generates time varying data for the capillary outflow density, pressure, temperature, species composition, and total capillary ablated mass. Outflow velocity is assumed to be sonic as a boundary condition in the hydrodynamic model. The profile of the outflow pressure closely follows that of the discharge current. Fig. 1 shows a polynomial fit to an experimental current profile and the resulting outflow pressure and plasma temperature, T_e, over a 220 μs discharge. The primary accomplishment of this model is it's ability to accurately reproduce or predict the total ablated mass, and time varying outflow pressure and species composition.

III. Plasma-Air Chemistry

During the capillary discharge, the generated plasma exits the capillary nozzle and either comes into immediate contact with the propellant, or expands in an open air filled chamber before encountering the propellant bed, depending on the propellant packing option being used [2], [10]. Our simulations indicate that, for typical ETC conditions, if the plasma jet is allowed to expand into air, plasma-air chemistry will occur if the capillary-propellant distance is less than approximately 10 mm [5]. For geometries with plasma-air interaction regions on this scale, plasma-air chemistry should be taken into account.

A plasma-air chemistry model based on previous experimental and theoretical work was developed that includes 20 species

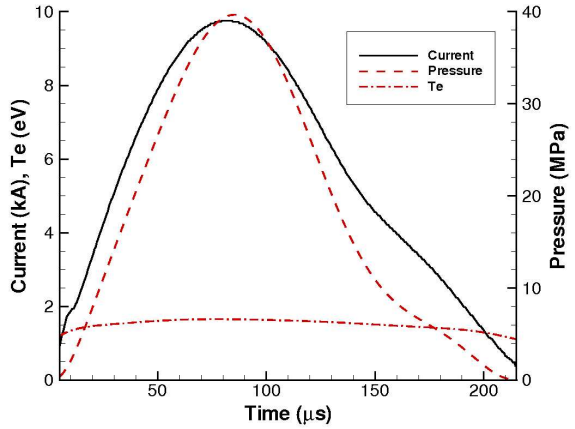

Fig. 1. Example input and output (dashed lines) from the capillary model, taken from [5].

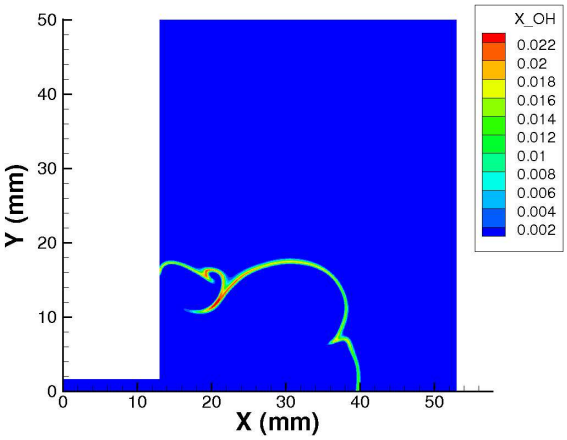

Fig. 2. Mole fraction of OH in the plasma jet, taken from [5]. Production is limited to a thin plasma-air reaction region at the periphery of the expanding jet.

and 41 chemical reactions [5]. This model was used in a chemically reacting CFD code developed at the University of Michigan, known as LeMANS. LeMANS is a parallelized, implicit Navier-Stokes CFD code that uses a modified Steger-Warming Flux Vector Splitting scheme for calculation of inviscid fluxes between mesh volumes, is second order accurate in space, with time integration performed using a point implicit method [11], [12]. The species included in the chemistry model are N_2, O_2, NO, N, O, OH, CO, CO_2, H_2O, CH, HCO, NH, H_2, C, H, H^+, C^+, N^+, O^+, and electrons. Electron impact ionization is assumed. The output from the capillary model (Section II) is used as time varying input to LeMANS. Electron mobility is limited in the model to ensure quasi-neutrality is maintained everywhere in the simulation. Fig. 2 shows a representative plasma-air chemistry result from the axisymmetric plasma jet simulation. We can see that the production of OH occurs in a thin region where the hydrogen of the expanding plasma jet encounters the oxygen in the ambient air, as predicted by theory. As the plasma jet expands, this reaction region is pushed outward. The sickle-like shape near X=20 mm, Y=10 mm is a recirculation region [5].

As part of the plasma-air study, a bayonet tube was simulated that approximated the physical dimensions used in [10]. A bayonet tube is inserted into a cylindrical bore in a propellant block. The tube has holes spaced along it's length which provide controlled ignition sites and allows ignition to occur not only at the end of the propellant closest to the capillary, but at the far end as well. Data from the simulated "holes" clearly shows that by the time the plasma wave reaches the end of the tube a significant amount of plasma-air chemistry has occurred. This indicates that in a bayonet tube-like packing configuration the ignition mechanism at one end of the tube may be different from the mechanism at the other end, due to the drastically different plasma chemical composition [5].

One of the main benefits of the plasma-air CFD studies is the ability to predict the plasma jet chemical composition under different geometries and capillary inflow conditions. Experimental attempts to measure the composition of the plasma jet have yielded few promising results [5]. The results of the simulations clearly indicate that small capillary-propellant distances allow us to entirely neglect plasma-air chemistry, which yields insight when choosing propellant packing options for practical ETC application.

IV. Plasma-Propellant Interaction Model

The primary focus of the ETC model is the simulation of the plasma-propellant interaction (PPI). This is accomplished via a kinetic theory based ablation model adapted from work by Keidar *et al* [9]. To model a propellant we require the vapor pressure, enthalpy of sublimation (ΔH), specific heat at constant pressure (C_p), the thermal conductivity (λ) and diffusivity (α). Simulations [6] were run comparing two propellants under consideration for ETC application. JA2 is a double-base propellant, which is optically semi-transparent, allowing radiation to penetrate in-depth. XM39 is a nitramine composite propellant, is optically opaque to most wavelengths, and does not allow significant radiation penetration.

For the PPI study, a range of plausible bulk plasma densities are chosen. Plasma number density (n_o) ranged from 10^{21}–10^{24} m^{-3}. The ablation model is similar to that used in the capillary model (Section II), with the ablation rate being a function of bulk plasma density and propellant surface temperature. Surface temperature is obtained via a one-dimensional thermal model representing the propellant bed. Experimental data was available for total ablated mass of a small propellant disc after exposure to a capillary plasma jet, this experimental geometry was used in the thermal model [13]. The propellant disc was of thickness $L = 4$ mm and was positioned in a sample holder taken to be a thermal sink. It is assumed that the experiment was conducted at one atmosphere pressure and initial temperature of $T_o = 298$ K. The thermal model and boundary conditions are

$$\partial_t T(x,t) = \alpha \partial_x^2 T(x,t),$$
$$T(0,t) = T_o,\ T(x,0) = T_o, \tag{3}$$

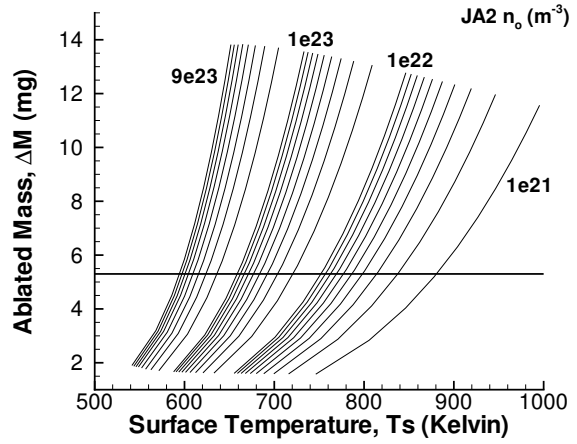

Fig. 3. Plasma-propellant interaction results for ablated mass versus propellant surface temperature for JA2, taken from [6].

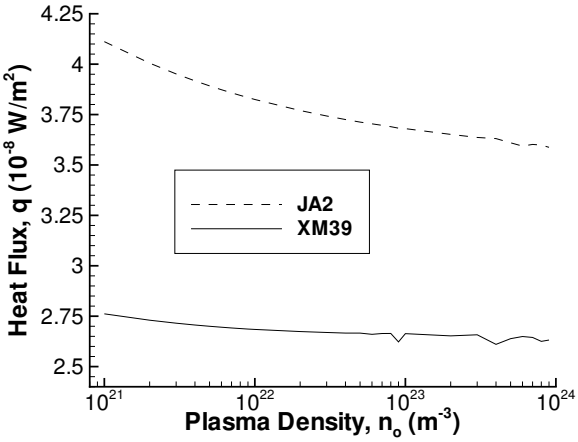

Fig. 4. Constant surface heat flux necessary to reproduce the experimental ablated mass as a function of bulk plasma density [6].

$$\partial_x T(L,t) = -\lambda^{-1}(q - \Delta H \Gamma - C_p(T_s - T_o)\Gamma),$$

where $T_s = T(L,t)$, and q is the surface heat flux to the propellant, which is assumed constant in time and space. The objective of the model is the determination of the effective surface heat flux over the course of the discharge, q. The resulting data can be presented as plots of total propellant ablated mass as a function of peak propellant surface temperature, at different bulk plasma densities, as in Fig. 3. Note that there are multiple solutions for each plasma density in terms of the peak surface temperature. Knowing the experimentally determined ablated mass allows us to determine the necessary heat flux as a function of plasma density. The experimental ablated mass for JA2 of 5.3 mg is presented as a horizontal line in Fig. 3. Fig. 4 presents data from the model that matches the experimental ablated masses for JA2 and XM39, representing the constant surface heat flux necessary to match the experimental results. We consider the ability to determine the exact bulk plasma density when we discuss model integration in Section VII.

The plasma-propellant interaction model led to several interesting conclusions. Fig. 4 clearly shows that JA2 will con-

sistently have a higher heat flux than XM39. Fig. 3 and the corresponding plot for XM39 show that XM39 has a higher surface temperature than JA2 at a fixed plasma density [6]. The downward trend in Fig. 4 is caused by the fact that as plasma density increases, the heat flux must decrease in order to match the experimental ablated mass, clearly illustrated by examining ablation rate contours [6]. Of significant interest is the difference between the two heat fluxes in Fig. 4. If the capillary generates an identical plasma at each firing (a valid assumption) then why is the total heat flux different? The most plausible explanation involves the propellant's optical properties. JA2's ability to access plasma radiation as a heat source allows it to tap into more of the available thermal energy of the plasma, while XM39's opacity reflects most of this radiative energy back into the plasma. It is also possible that plasma surface chemistry is responsible for part of this difference, and is being explored currently, as we will discuss in Section VI.

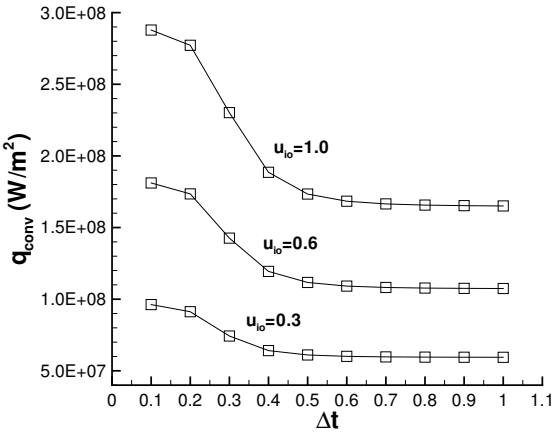

Fig. 5. Convective heat flux to XM39 for $n_o = 3 \times 10^{22} m^{-3}$ for different ion inflow velocities, taken from [7].

V. Collisional Plasma Sheath Model

The work modeling the plasma-propellant interaction yielded the total heat flux incident on the propellant surface [6]. In order to determine what phenomena contribute to the total heat flux, a collisional plasma sheath model was developed to find the convective heat flux to the propellant bed [7].

A plasma sheath develops at any plasma-solid interface. High speed electrons strike the propellant before the slower, heavier ions, causing a negative potential to build up on the propellant. This negative potential grows until the electron and ion fluxes balance, and a floating potential is reached. This plasma sheath causes ions to accelerate as they approach the wall due to the potential field, thus increasing their kinetic energy. Ion-neutral collisions in the sheath decrease the ion drift velocity, decreasing the ion kinetic energy. These two factors determine the convective ion flux to the propellant bed in ETC application.

The one-dimensional sheath model assumes Boltzmann electrons, a single fluid ion species, and a uniform neutral background density. The neutral density is found from the PPI model, where the neutral number density is given by $n_n = P_V(T_s)/(kT_s)$, where $P_V(T_s)$ is the propellant vapor pressure at surface temperature T_s, as determined by the PPI thermal model [6]. In the results presented here, a bulk plasma temperature of $T_e = 1.5$ eV is assumed. The only remaining unknown is the velocity of the ions as they enter the sheath. Theoretical limits for a collisional plasma sheath indicate that the inflow velocity should be less than or equal to the Bohm velocity, given as $C_s = \sqrt{eT_e/m_i}$, where m_i is the ion mass. We non-dimensionalize the inflow velocity as $u_{io} = V_{io}/C_s$, and select representative values of u_{io} =0.3, 0.6, and 1.0. The convective heat flux to the propellant bed is given as

$$q_{conv} = (n_o C_s u_{io}) \left(\frac{m_i}{2} (C_s u_{iw})^2 + 2eT_e - eT_e \eta_w \right), \quad (4)$$

where n_o is the bulk plasma number density, and η_w is the non-dimensional floating potential, calculated via an analytical expression [7]. The only unknown in (4) is u_{iw}, the non-dimensional ion-wall impact velocity, which we obtain from the sheath solution.

Fig. 5 shows the convective heat flux to XM39 for a bulk plasma density of $n_o = 3 \times 10^{22} m^{-3}$ and different ion inflow velocities, where $\Delta t = 1$ is the length of the plasma pulse from the PPI work of Section IV. We can see that the convective heat flux changes curvature in Fig. 5, and appears to approach a limit near $\Delta t = 0$, and clearly reaching a different limit well before $\Delta t = 1$. The two extremes are the collisionless and fully collisional plasma sheath limits. Analytical expressions exist for the ion-wall impact velocities for both fully collisional and collisionless plasma sheaths; these analytical limits are shown in Fig. 6 for the $u_{io} = 1$ case. During the early portion of the discharge, the propellant surface temperature, and thus the neutral density, is low, resulting in a low collisionality in the sheath. By the end of the pulse the neutral density is high enough that the sheath is fully collisional. However, the sheath remains in a transition regime for most of the plasma pulse. Since JA2 has a higher ablated mass, results for that propellant typically do not come as close to the collisionless limit as do the results for XM39.

The main conclusions from the collisional plasma sheath model include the fact that XM39 receives a higher convective heat flux than JA2 for a given plasma density and ion inflow velocity. Given that the PPI model shows that JA2 has a higher total heat flux, this means that JA2 receives enough plasma radiation to overcome XM39's higher convective heat flux, indicating that plasma radiation is a significant heat transport mechanism in the PPI. As in the PPI model, the bulk plasma density, n_o, is treated as a parameter as it is not known at this time. We find that, depending on the value of the bulk plasma density, convective heat flux can represent a significant portion of the total heat flux to the propellant bed [7].

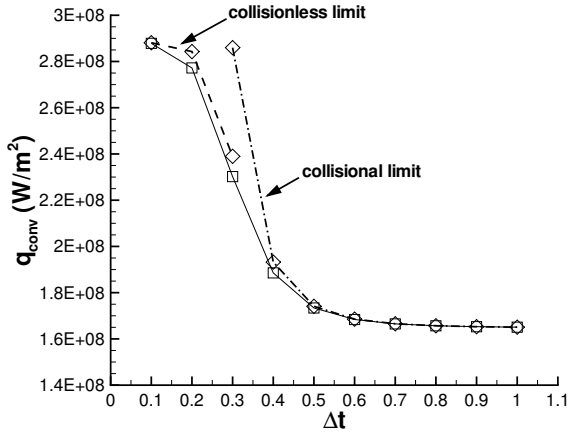

Fig. 6. Comparison of simulation result to limits for collisionless and fully collisional ion-wall impact velocity, taken from [7].

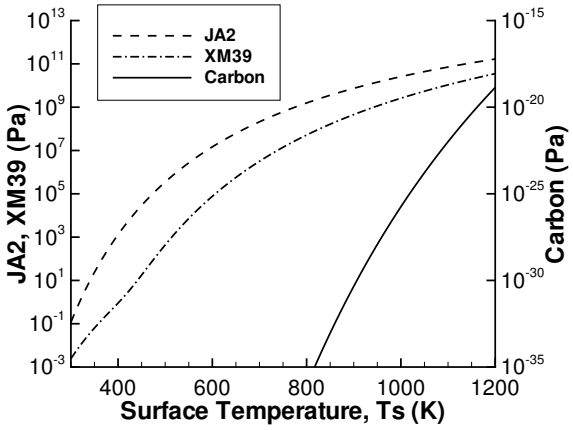

Fig. 7. Vapor pressure of JA2, XM39, and carbon as a function of surface temperature [6], [15]. Note that the carbon vapor pressure is negligible when compared to that of the propellant.

VI. Surface Chemistry

Current work on the ETC model is focused on adding surface chemistry effects to the PPI model and final integration of all the submodels (Sections II-V). The focus of the investigation into surface chemistry phenomena is carbon film deposition on the propellant surface. The propellants are composed primarily of carbon, hydrogen, oxygen and nitrogen. Experimental ablation studies frequently show carbon deposition to the surface of the ablated material [14]. Carbon deposition to the propellant surface will affect the ablation rate in two ways. First, the ablation of propellant will decrease, as the carbon film forms a patchy covering on the propellant which shields exposure to the plasma. Secondly, as carbon attaches itself to the propellant, or to the already existing carbon film, a new chemical bond is formed which extracts energy from the material surface. This energy loss can be accounted for in the thermal boundary condition in (3). The energy lost in this way will decrease the propellant surface temperature, causing a further decrease in the ablation rate.

As a first step toward implementing film deposition in the PPI model, the ablation rate for carbon was found via the ablation model used in Sections II and IV, which is based on the material vapor pressure. It was found for the surface temperature range predicted by the PPI model (300 K $\leq T_s \leq$ 1200 K) and for the conditions of the experiment used to fix the total ablated mass [6], [13], that carbon ablation is negligible. This is due to carbon's low vapor pressure in the temperature range. Fig. 7 shows the vapor pressure of JA2 and XM39, taken from [6], compared to that of carbon, taken from [15], over the temperature range of interest. We see that the carbon vapor pressure is much less than the vapor pressure of either JA2 or XM39, resulting in negligible carbon ablation.

The rate of carbon film growth is thus the critical aspect of the model, as any carbon that is deposited will not re-ablate during the PPI. Typically, the amount of material deposited back onto the ablating surface is calculated using a fitting parameter [4]. The ability to use a fitting parameter does not present itself here, thus we must model this in some way. One approach being considered is to use the carbon-carbon bonding energies and rates to estimate a probability that a carbon atom will attach to the propellant surface, forming a film. These efforts are currently underway.

VII. Model Integration

Here we discuss the integration of all submodels into an end-to-end ETC model. As we have seen from Section IV, the PPI model requires the plasma density at the propellant surface. Previously, this information was not available, and a parametric approach was used, as shown in Fig. 4. It thus became a high priority to determine the exact plasma density at the propellant surface. This is to be done by one of two different methods, depending on the propellant packing option used. Either the capillary nozzle is in direct (or near direct) contact with the propellant surface, in which case the capillary output can be used directly to find the plasma density, or the capillary-propellant distance is greater than approximately 10 mm, in which case the plasma-air chemistry model should be used to determine the plasma density, especially if there is a large chamber which allows the plasma jet to undergo expansion. Although the former option is most likely in practical ETC application, we must still use the experimental ablated mass to fix the total heat flux in the PPI model, and that data comes from expanding plasma jet studies [13]. Thus we will use the CFD plasma-air chemistry model to determine the plasma density at the propellant surface, keeping in mind that using the capillary model to find the plasma density directly is simpler in comparison.

Note that the PPI results were utilized in the convective heat flux model (Section V), meaning that if the plasma density and total heat flux are known, then the convective heat flux will also be known. The surface chemistry model described in Section VI will, through the energy loss term in the thermal model, decrease the total heat flux to the propellant bed, although

by how much is not clear at this time. The PPI model will readily accommodate a time varying plasma density, and using the experimental ablated mass we will obtain a more accurate result for the total heat flux. The surface temperature versus time profile generated by the PPI thermal model can then be used in the convective heat flux model to determine exactly how important convective heating is in the PPI by allowing us to calculate the exact ratio of convective to total heat flux.

VIII. Conclusion

Presented was the progress toward an end-to-end electrothermal chemical gun model. The model covers the generation of the plasma in the capillary plasma source, the plasma-air interaction of the expanding plasma jet, and the plasma-propellant interaction leading up to propellant ignition. The model yields good results when compared to existing theoretical and experimental limits. The results of the various simulations yield insight into the design of practical electrothermal chemical guns. Near term additions to the model and integration of all submodels are also discussed.

References

[1] A. Koleczko, W. Ehrhardt, S. Kelzenberg, and N. Eisenreich, "Plasma ignition and combustion", *Prop. Explos. Pyrotech.*, vol. 26, pp. 75-83, 2001.

[2] J. Dyvik, J. Herbig, R. Appleton, J. O'Reilly, and J. Shin, "Recent Activities in Electrothermal Chemical Launcher Technologies at BAE Systems", *IEEE Trans. on Magnetics*. vol. 43, no. 1, pp. 303-307, January 2007.

[3] M. Keidar, and I. D. Boyd, "Ablation study in the capillary discharge of an electrothermal gun", *Journal of Applied Physics*, vol. 99, 053301, 2006.

[4] M. Keidar, I. D. Boyd, A. Williams, and R. Beyer, "Ablation Study in a Capillary Sustained Discharge", *IEEE Transactions on Magnetics*, vol. 43, no. 1, pp. 308-312, January 2007.

[5] A. J. Porwitzky, L. C. Scalabrin, M. Keidar, and I. D. Boyd, "Chemically Reacting Plasma Jet Expansion Simulation for Application to Electrothermal Chemical Guns", *38th AIAA Plasmadynamics and Lasers Conference*, Miami, Florida, 25-28 June 2007.

[6] A. J. Porwitzky, M. Keidar, and I. D. Boyd, "Modeling of the Plasma-Propellant Interaction", *IEEE Trans. on Magnetics*. vol. 43, no. 1, pp. 313-317, January 2007.

[7] A. J. Porwitzky, M. Keidar, and I. D. Boyd, "On the Mechanism of Energy Transfer in the Plasma-Propellant Interaction", *Propellants, Explosives, Pyrotechnics*. vol. 32, no. 5, pp. 385-391, October 2007.

[8] M. Keidar, J. Fan, I. D. Boyd, and I. I. Beilis, "Vaporization of heated materials into discharge plasmas", *Journal of Applied Physics*. vol. 89, pp. 3095, 2001.

[9] M. Keidar, I. D. Boyd, and I. I. Beilis, "On the model of Teflon ablation in an ablation-controlled discharge", *Journal of Physics D*. vol. 34, pp. 1675, 2001.

[10] R. Beyer, A. L. Brant, "Plasma Ignition in a 30-mm Cannon", *IEEE Trans. on Magnetics*. vol. 43, no. 1, pp. 294-298, January 2007.

[11] L. C. Scalabrin, and I. D. Boyd, "Development of an Unstructured Navier-Stokes Solver For Hypersonic Nonequilibrium Aerothermodynamics", *38th AIAA Thermophysics Conference*, 6-9 June 2005, Toronto, Canada.

[12] L. C. Scalabrin, and I. D. Boyd, "Numerical Simulation of Weakly Ionized Hypersonic Flow for Reentry Configuations", *9th AIAA/ASME Joint Thermophysics and Heat Transfer Conference*, 5-8 June 2006, San Francisco, California.

[13] J. Li, T. A. Litzinger, and S. Thynell, "Interaction of Capillary Plasma with Double-Base and Composite Propellants," *Journal of Propulsion and Power*, vol. 20, no. 4, July-August 2004.

[14] M. Keidar, I. D. Boyd, E. L. Antonsen, F. S. Gulczinski III and G. Spanjers, "Propellant Charring in Pulsed Plasma Thrusters," *Journal of Propulsion and Power*, vol. 20, no. 6, November-December 2004.

[15] F. R. Leider, O. H. Krikorian, and D. A. Young, "Thermodynamic Properties of Carbon Up To The Critical Point," *Carbon*, vol. 11, pp. 555-563, 1973.